

Supplementary Materials for

Interplay of m⁶A and H3K27 trimethylation restrains inflammation during bacterial infection

Chenglei Wu, Weixin Chen, Jincan He, Shouheng Jin, Yukun Liu, Yang Yi, Zhuoxing Gao, Jiayan Yang, Jianhua Yang*, Jun Cui*, Wei Zhao*,

*Corresponding author. Email: zhaowei23@mail.sysu.edu.cn (W.Z.); cuij5@mail.sysu.edu.cn (J.C.); yangjh7@mail.sysu.edu.cn (Jianhua Yang)

Published 19 August 2020, *Sci. Adv.* **6**, eaba0647 (2020)
DOI: 10.1126/sciadv.aba0647

The PDF file includes:

Figs. S1 to S7
Table S1
Legends for data files S1 and S2

Other Supplementary Material for this manuscript includes the following:

(available at advances.sciencemag.org/cgi/content/full/6/34/eaba0647/DC1)

Data files S1 and S2

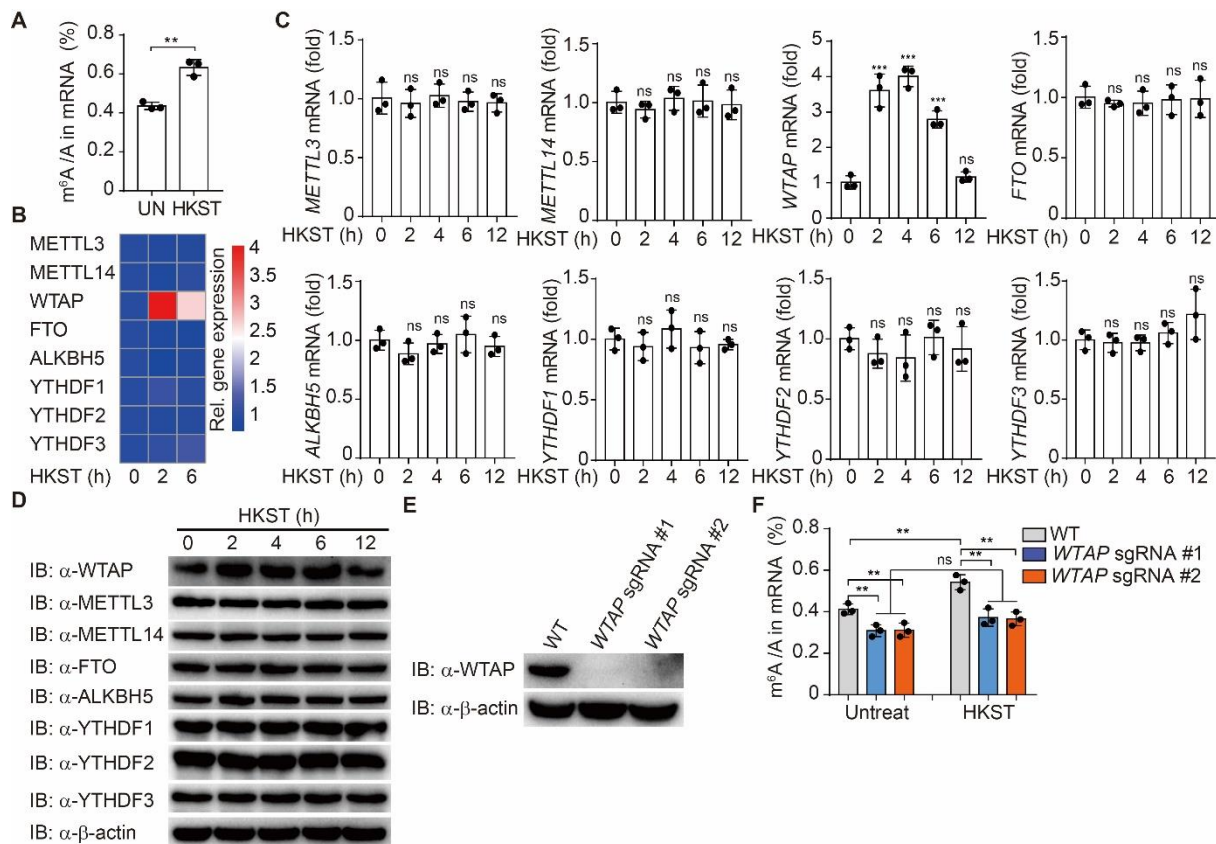


fig. S1. Expression of WTAP is upregulated during bacterial infection. (A) THP-1 cells were exposed to HKST, and the m⁶A level on poly(A) RNA was quantified using an m⁶A RNA methylation detection kit. (B) RNA-seq analyses showing the relative mRNA expression levels of genes encoding for m⁶A modulators in THP-1 cells upon HKST treatment. (C) Real-time PCR analyses for mRNA expression of the genes encoding for m⁶A modulators in THP-1 cells upon HKST treatment. (D) Immunoblot analysis of m⁶A modulators in THP-1 cells stimulated with HKST. (E) Immunoblot analysis of cell extracts from wild-type (WT) and *WTAP* knockout (KO) THP-1 cells with the indicated antibodies. (F) WT and *WTAP* KO THP-1 cells were exposed to HKST, and the m⁶A levels on poly(A) RNA were quantified using an m⁶A quantification kit. Data (A, C and F) are combined from three individual experiments with triplicate and presented as means \pm SEM. **P* < 0.05, ***P* < 0.01, and ****P* < 0.001 compared to control cells (Student's t-test). Data (D and E) are representatives of three independent experiments with similar results. Representative blots are shown.

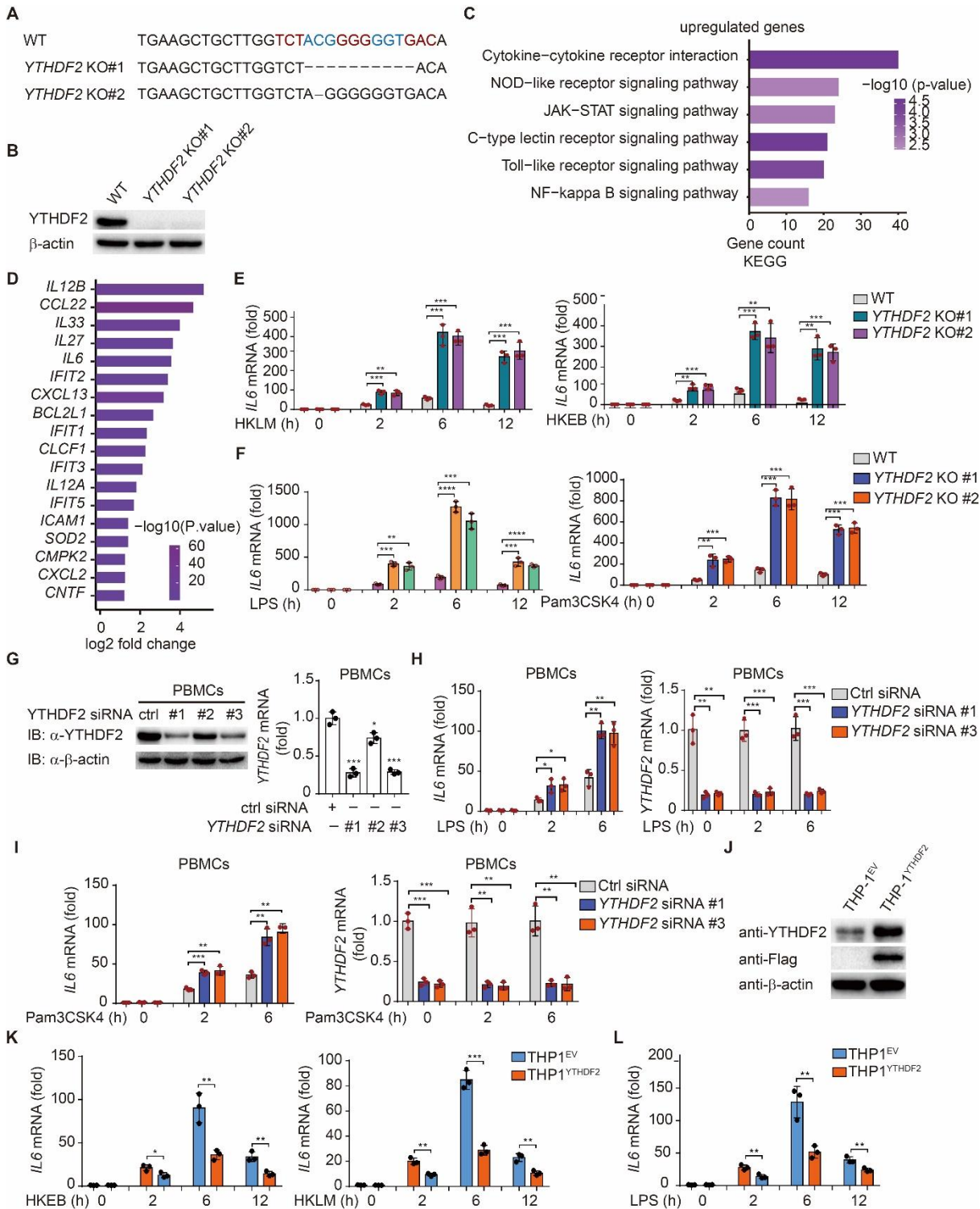


fig. S2. YTHDF2 inhibits the transcription and production of IL-6. (A and B) Sequence and immunoblotting analysis of WT and *YTHDF2* knockout (KO) THP-1 cells. (C) Kyoto Encyclopedia of Genes and Genomes (KEGG) analysis of the 1,606 upregulated genes in *YTHDF2* KO cells, compared to those in wild type (WT) cells after HKST infection. (D) Fold change of inflammatory related genes mRNA expression in *YTHDF2* KO cells versus WT THP-1 cells with HKST stimulation according to RNA-seq data. (E) WT and *YTHDF2* KO THP-1 cells were infected

with HKLM or HKEB for indicated periods, then analyzed by real-time PCR for *IL-6* transcription. **(F)** WT and *YTHDF2* KO THP-1 cells were stimulated with LPS (200 ng/ml) or Pam3CSK4(100 ng/ml) for indicated periods, then analyzed by real-time PCR for *IL-6* transcription. **(G)** Immunoblotting and real-time PCR analysis of *YTHDF2* in PBMCs transfected with the indicated *YTHDF2* siRNAs. **(H and I)** PBMCs were transfected with *YTHDF2* siRNAs or control siRNA for 48 h. These cells were stimulated with LPS (200 ng/ml) and Pam3CSK4 (100 ng/ml) for indicated periods and analyzed by real-time PCR for *IL6* and *YTHDF2* expression. **(J)** Immunoblot analysis of *YTHDF2* in wild type (WT) THP-1 cells stably expressing the empty vector (THP-1^{EV}) or Flag-tagged *YTHDF2* (THP-1^{YTHDF2}). **(K and L)** THP-1^{EV} and THP-1^{YTHDF2} cells were stimulated with HKEB, HKLM and LPS (200 ng/ml) for indicated periods and detected *IL-6* expression by real-time PCR. Data **(A, E, F, G, H, I and K, L)** are combined from three individual experiments with triplicate and presented as means \pm SEM. *P < 0.05, ** P < 0.01, and *** P < 0.001 compared to control cells (Student's t-test). Data **(B, G and J)** are representatives of three independent experiments with similar results. Representative blots are shown.

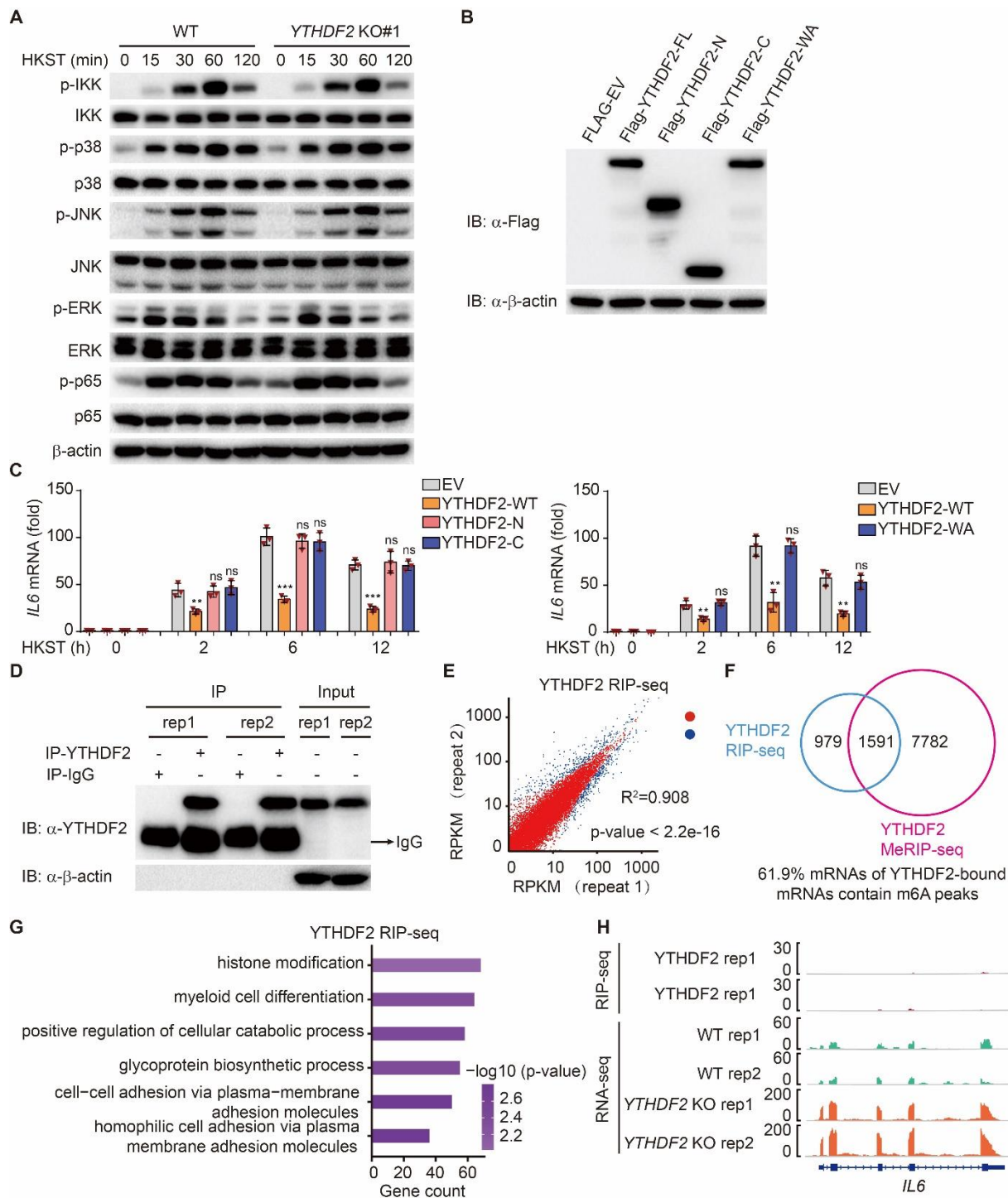


fig. S3. YTHDF2 functions as m⁶A reader to bind to histone modification associated genes.

(A) Wild type (WT) and *YTHDF2* knockout (KO) THP-1 cells were stimulated with HKST for indicated periods, then the cell lysates were analyzed by immunoblot indicated antibodies. (B) Immunoblotting analysis of cell extracts from THP-1 cells stably expressing Flag-tagged full-length *YTHDF2* (FL), *YTHDF2* N/C-terminal truncation mutants or the sites mutant. (C) THP-1^{EV}, THP-1^{YTHDF2-FL}, THP-1^{YTHDF2-N}, and THP-1^{YTHDF2-C} cells and THP-1^{YTHDF2-WA} cells were treated with HKST in different time points, then analyzed *IL-6* transcription by real-time PCR. (D) THP-1 cells

were exposed to for 6 h, and the cell lysates were subjected to RNA immunoprecipitation (RIP) with an anti-YTHDF2 antibody or control IgG, followed by immunoblotting with indicated antibodies. **(E)** Correlation matrix plot of two replicates of YTHDF2-RIP-seq samples. **(F)** Overlap of transcripts identified by RIP-seq of YTHDF2 and m⁶A-seq data in HKST stimulated THP-1 cells. **(G)** GO analysis of most enriched YTHDF2-bound mRNA in infected THP-1 cells from YTHDF2-RIP-seq data. **(H)** Genome browser tracks showing *IL6* transcript reads from RIP-seq and RNA-seq data. Data **(A, B and D)** are representatives of three independent experiments with similar results. Data **(C)** are plotted as mean \pm SEM of combined from three independent experiments with triplicate. *P < 0.05, ** P < 0.01, and *** P < 0.001 compared to control cells (Student's t-test).

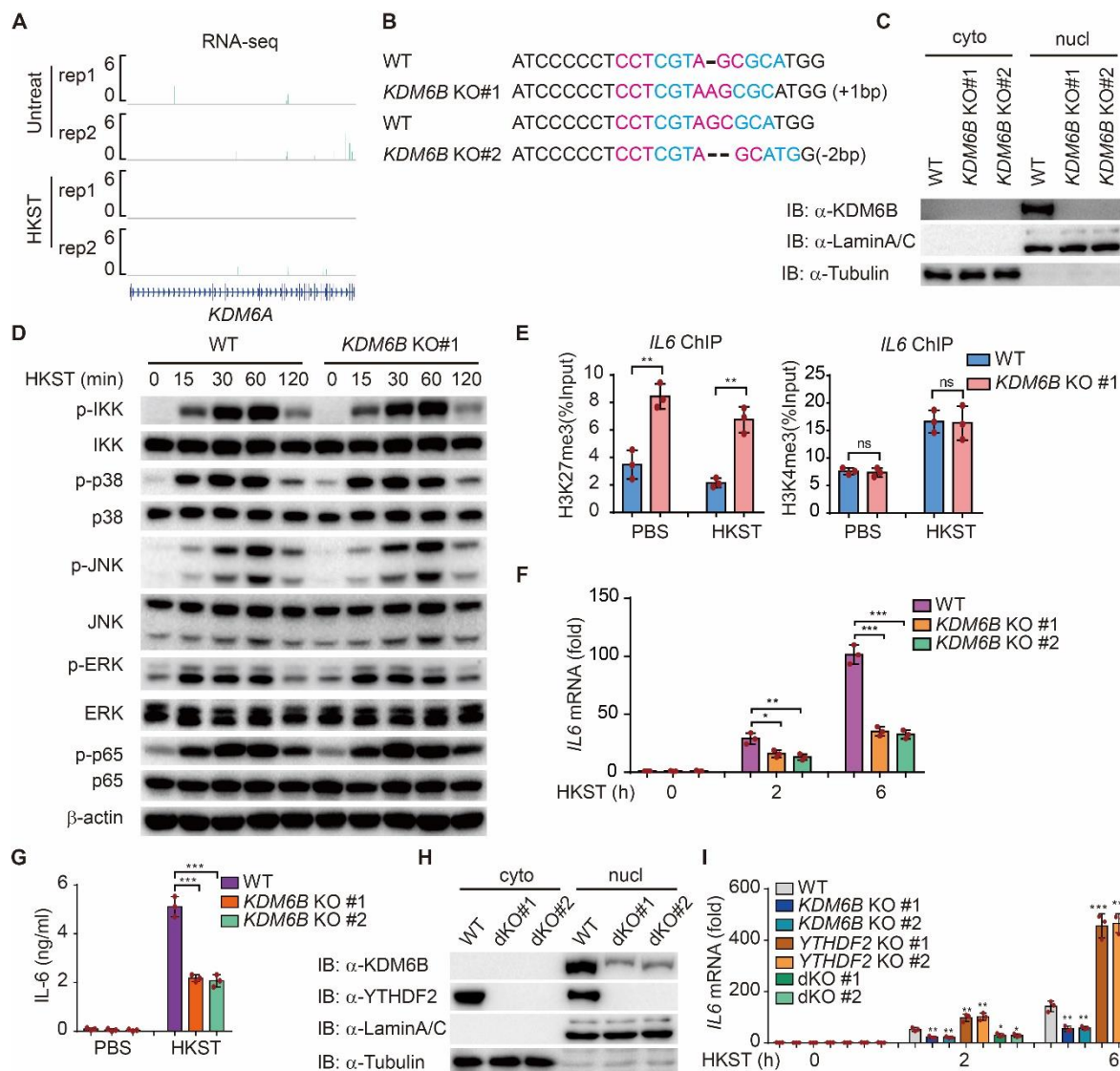


fig. S4. YTHDF2 decreases the transcription of *IL6* in a *KDM6B*-dependent manner. (A) Genome browser tracks showing *KDM6A* transcript reads from RNA-seq data. (B and C) Sequence and immunoblotting analysis of cells extracts from wild type (WT) and *KDM6B* knockout (KO) THP-1 cells. (D) WT and *KDM6B* KO THP-1 cells were stimulated with HKST for indicated periods, then the cell lysates were analyzed by immunoblot with indicated antibodies. (E) ChIP-qPCR assay for H3K27me3 and H3K4me3 at *IL-6* gene promoter loci in WT and *KDM6B* KO THP-1 cells in response to HKST or not. (F) The transcription of *IL6* measured by real-time PCR in WT and *KDM6B* KO THP-1 cells treated with HKST for indicated periods. (G) WT and *KDM6B* KO cells were stimulated with HKST for 24 h before the supernatants were collected. The production of IL-6 was analyzed by ELISAs. (H) Generate *KDM6B* and *YTHDF2* double knockout (dKO) THP-1 cell lines. (I) The transcription level of *IL-6* were analyzed by real-time PCR in WT, *KDM6B* KO, *YTHDF2* KO, or dKO THP-1 cells infected with HKST for the indicated periods. Data (D and H) are representatives of three independent experiments with similar results. Data (E

to **G** and **I**) are plotted as mean \pm SEM of combined from three independent experiments with triplicate. *P < 0.05, ** P < 0.01, and *** P < 0.001 compared to control cells (Student's t-test).

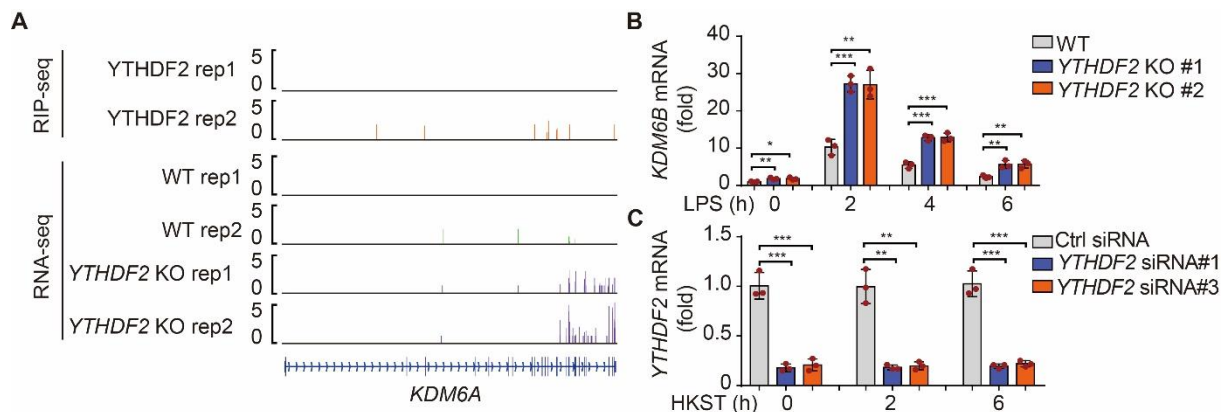


fig. S5. YTHDF2 decays *KDM6B* transcript. (A) Genome browser tracks displaying YTHDF2-RIP-seq (upper panels, two replicates) and RNA-seq (lower panels, two replicates) reads distribution in *KDM6A* mRNA of wild type (WT) and *YTHDF2* knockout (KO) THP-1 cells with HKST infection. (B) WT and *YTHDF2* KO THP-1 cells were stimulated with LPS (200 ng/ml) for indicated periods, then analyzed by real-time PCR for *KDM6B* transcription. (C) Transfected the indicated *YTHDF2* siRNA into PBMCs for 24h, and analyzed *YTHDF2* expression after stimulated with HKST for indicated periods. Data (B and C) are combined from three individual experiments with triplicate and presented as means \pm SEM. * $P < 0.05$, ** $P < 0.01$, and *** $P < 0.001$ compared to control cells (Student's t-test).

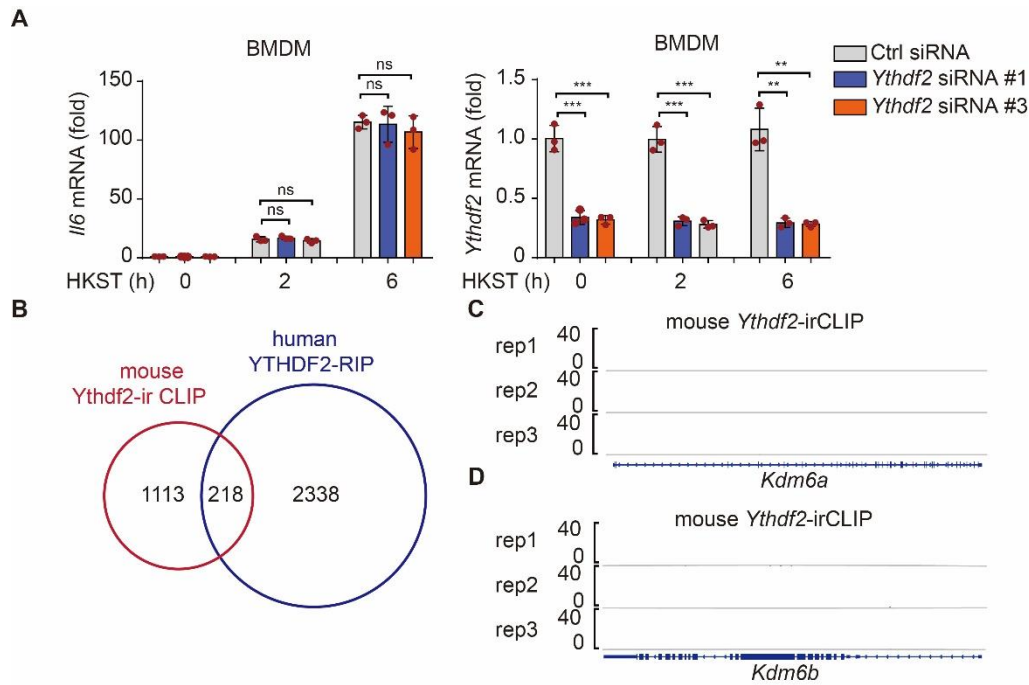


fig. S6. The regulation of Il-6 production by Ythdf2 is not conserved in mice. (A) Murine bone marrow derived macrophages (BMDMs) that were transfected with *Ythdf2* siRNAs or control siRNA for 48h were stimulated with HKST for indicated periods, then analyzed by real-time PCR for *Il6* and *Ythdf2* expression. (B) Venn diagram displaying that there were a few overlapped transcripts bound to YTHDF2 between human and mouse according infrared crosslinking-immunoprecipitation-sequencing (irCLIP-seq) data and RIP-seq data. (C and D) IGV browser tracks of *Kdm6a* and *Kdm6b* mRNA in mouse *Ythdf2*-irCLIP data. Data (A) are combined from three individual experiments with triplicate and presented as means \pm SEM. * $P < 0.05$, ** $P < 0.01$, and *** $P < 0.001$ compared to control cells (Student's t-test).

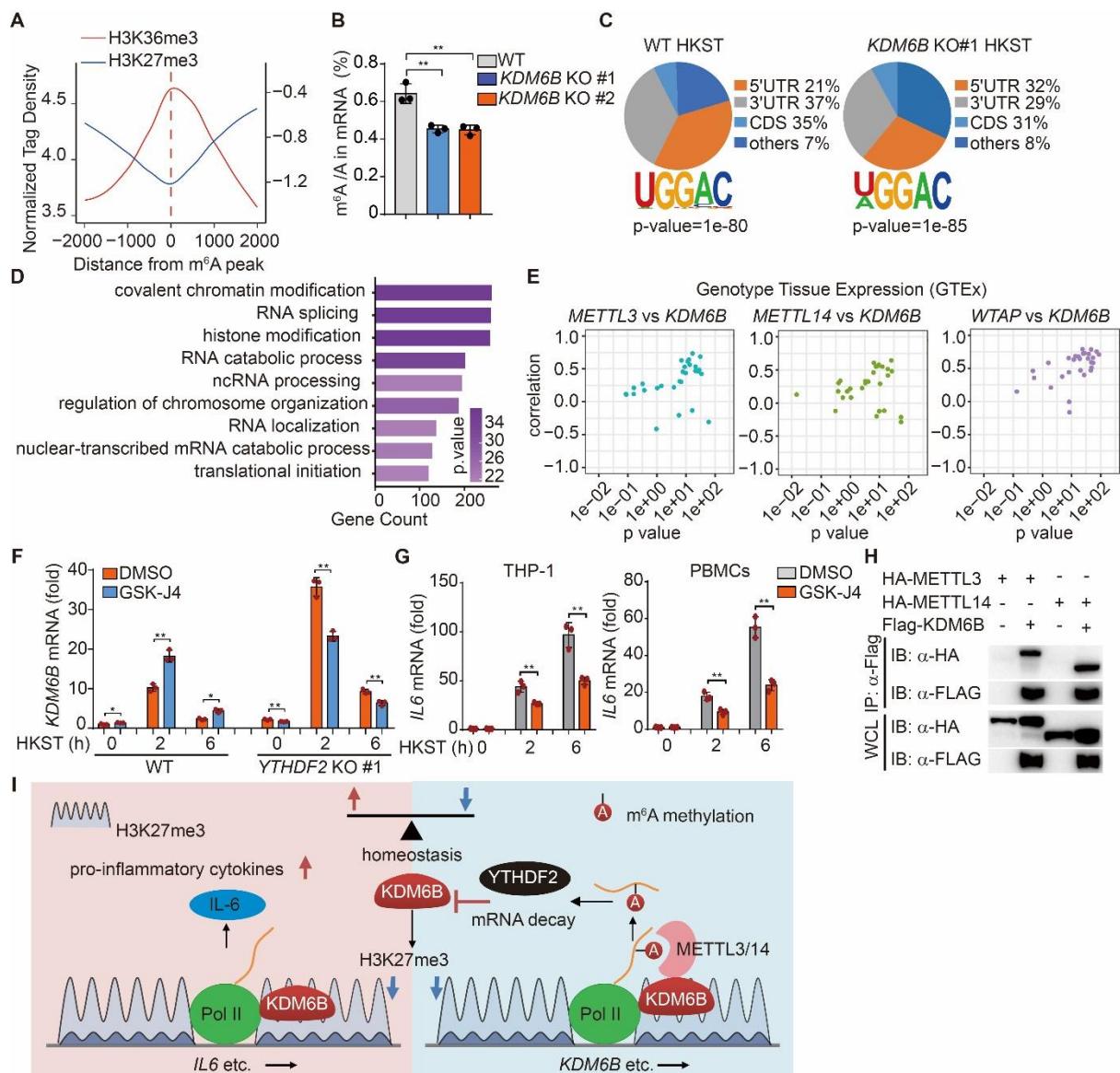


fig. S7. KDM6B promotes m⁶A modification via recruiting m⁶A methyltransferase complex. (A) Distance of H3K27me3 and H3K36me3 signals to the nearest m⁶A peaks. (B) WT and *KDM6B* KO THP-1 cells were exposed to HKST, and the m⁶A level on poly(A) RNA was quantified using an m⁶A RNA methylation detection kit. (C) Pie chart depicting the proportion of m⁶A peak distribution in the 5'UTR, CDS, and 3'UTR regions in WT and *KDM6B* KO THP-1 cells infected with HKST. (D) GO analysis of genes that contained hypomethylated m⁶A peaks in HKST infected *KDM6B* KO THP-1 cells compared with WT THP-1 cells. (E) Correlation of *KDM6B* with individual m⁶A methyltransferase complex genes (that is, *METTL3*, *METTL14* and *WTAP*) in expression in normal tissues. (F) WT or *YTHDF2* KO THP-1 cells were treated with DMSO or GSK-J4 for 24h, and then infected with HKST for indicated periods. The transcription of *KDM6B* mRNA was measured by real-time PCR. (G) Detection of the transcription of *IL6* by real-time PCR in THP-1 cells or PBMCs treated with DMSO or GSK-J4 exposed to HKST for indicated periods.

(H) HeLa cells were transfected with HA-tagged *METTL3* or *METTL14* and Flag-tagged *KDM6B*. The cell lysates were subjected to immunoprecipitation with anti-Flag antibodies and immunoblotted with the indicated antibodies. **(I)** A Schematic model illustrating how YTHDF2 controls inflammatory response and how KDM6B facilitates m⁶A deposition via recruiting m⁶A methyltransferase complex. Data **(B, F and G)** are plotted as mean \pm SEM of combined three independent experiments with triplicate. *P < 0.05, ** P < 0.01, and *** P < 0.001 compared to control cells (Student's t-test). Data **(H)** are representatives of three independent experiments with similar results.

Supplementary Table 1. Oligos of this article

sgRNAs and siRNAs used for this study		
Human YTHDF2 sgRNA #1	GTGAAGCTGCTTGGTCTACG	
Human YTHDF2 sgRNA #2	TGAAGCTGCTTGGTCTACGG	
Human KDM6B sgRNA #1	ATCCCCCTCCTCGTAGCGCA	
Human KDM6B sgRNA #2	CCAGGCAGCCATGCGCTACG	
Human WTAP sgRNA #1	CTTGGGAAGAGGTTCTTCGT	
Human WTAP sgRNA #2	GCATATGTACAAGCTTTGGA	
Human YTHDF2 siRNA #1	sense:GUGCAUACAGUUUUCUCUA	
	anti-sense:CACGUAUGUCAAAAAGAGAU	
Human YTHDF2 siRNA #2	sense:CACUCCUACCAGAUGCAA	
	anti-sense:GUGAAGGAUGGUCUACGUU	
Human YTHDF2 siRNA #3	sense:CAGUGUUGGAGAAGCUUCG	
	anti-sense:GUCACAACCUCUUCGAAGC	
Mouse YTHDF2 siRNA #1	sense:GUGGGUCCAUCACUAGUAA	
	anti-sense:UUACUAGUGAUGGACCCAC	
Mouse YTHDF2 siRNA #2	sense:GGACAGCAGGCCAAUAAUA	
	anti-sense:UAUUAUUGGCCUGCUGUCC	
Mouse YTHDF2 siRNA #3	sense:CGGUCCAUUAUAACUUA	
	anti-sense:UAUAGUUAUUAUUGGACCG	
Primers of Real-time PCR		
Human IL-6	Forward	AGAGGCACTGGCAGAAAACAAC
	Reverse	AGGCAAGTCTCCTCATTGAATCC
Human KDM6B	Forward	TGATGCTAAGCGGTGGAAG
	Reverse	TGTTGATGTTGACGGAGCAG
Human ACTB	Forward	ACCATGTACCCTGGCATTGC
	Reverse	CGGACTCGTCATACTCCTGC
Human CCL22	Forward	ATCGCCTACAGACTGCACTC
	Reverse	GACGGTAACGGACGTAATCAC
Human IL12B	Forward	GCGGAGCTGCTACACTCTC
	Reverse	CCATGACCTCAATGGGCAGAC
Human METTL3	Forward	CATTGCCCACTGATGCTGTG
	Reverse	AGGCTTCTACCCCATCTTGA
Human METTL14	Forward	AGTGCCGACAGCATTGGTG
	Reverse	GGAGCAGAGGTATCATAGGAAGC
Human WTAP	Forward	CTTCCAAGAAGGTTTCGATTGA
	Reverse	TCAGACTCTCTTAGGCCAGTTAC
Human FTO	Forward	ACTTGGCTCCCTTATCTGACC

	Reverse	TGTGCAGTGTGAGAAAGGCTT
Human ALKBH5	Forward	AGTTCAGTTCAAGCCTATTCG
	Reverse	TGAGCACAGTCACGCTTCC
Human YTHDF1	Forward	ACCTGTCCAGCTATTACCCG
	Reverse	TGGTGAGGTATGGAATCGGAG
Human YTHDF2	Forward	CCTTAGGTGGAGCCATGATTG
	Reverse	TCTGTGCTACCCAACTTCAGT
Human YTHDF3	Forward	ACAAGTGGATCTCAGGGAC
	Reverse	GCTGAGGCTGCTGGATTAT
Human ICAM1	Forward	ATGCCCAGACATCTGTGTCC
	Reverse	GGGGTCTCTATGCCCAACAA
mouse Ythdf2	Forward	GAGCAGAGACCAAAAGGTCAAG
	Reverse	CTGTGGGCTCAAGTAAGGTTC
mouse Il6	Forward	TAGTCCTTCCCTACCCCAATTTCC
	Reverse	TTGGTCCTTAGCCACTCCTTC
Primers of ChIP-qPCR		
Human IL-6	Forward	ACTTCGTGCATGACTTCAGC
	Reverse	GCGGATCATGCTTTCTGTTGCCATGGTGTGTC
Human CCL22	Forward	CAGTCTTGAAGACTTGGAGTCTAGGATC
	Reverse	GATGGTGGGAGGGCAGCACC
Human IL-12B	Forward	TGTGTCTGTATGAAATGTGCATGGGTG
	Reverse	TGAGATGAAGGGCAAAGGGTTTAGTAC
Human ICAM1	Forward	TTGGCTAGATTGCGTCTCTTACAGTTTC
	Reverse	CAGAGCCAAGTTCCCAAACCATCATGATC
Human KDM6B	Forward	ACCCCTATCTCTGCCCCCTG
	Reverse	CTCCTTGGCCTGTGCGGG
Primers of MeRIP-qPCR		
Human KDM6B	Forward	AGAAGAGATCAGCCGGGCTTG
	Reverse	CAGCCTCCTCCTTGGCCTGTG
Primers of RIP-qPCR		
Human KDM6B	Forward	TGATGCTAAGCGGTGGAAG
	Reverse	TGTTGATGTTGACGGAGCAG

Data file S1. YTHDF2 RNA-seq

Data file S2. YTHDF2 RIP-seq